Synthesis, Characterization, and Molecular Structure of the New S_2O Complex $Mo(S_2O)(S_2CNEt_2)_3\cdot{}^1/_2Et_2O$

Malcolm A. Halcrow,[1] John C. Huffman,[2] and George Christou*,[1]

Department of Chemistry and Molecular Structure Center, Indiana University, Bloomington, Indiana 47405-4001

Received February 15, 1994®

The reaction of $[Mo(S_2)(S_2CNEt_2)_3]$ (**1**) with 1 equiv of *meta*-chloroperbenzoic acid (mCPBA) in CH_2Cl_2 at 0 °C yields $[Mo(S_2O)(S_2CNEt_2)_3]$ (**2**) in ~70% yield. Complex **2** crystallizes from $MeNO_2/Et_2O$ as the hemiether solvate in the monoclinic space group $C2/c$ with the following unit cell dimensions at –165 °C: a = 18.294(4) Å, b = 9.468(2) Å, c = 32.101(7) Å, β = 92.75(1)°, and Z = 8. A total of 2641 unique data with $F > 2.33\sigma(F)$ were refined to values of R and R_w of 3.99 and 3.89%, respectively. The structure of $\mathbf{2}\cdot{}^1/_2EtO$ shows a distorted pentagonal bipyramidal Mo center, with the S_2O ligand coordinated to an axial site in an asymmetric η^2-S,S′-fashion. The EPR and electronic spectra and electrochemical properties of **1** and **2** are very similar: for **1**, $\langle g\rangle = 1.977$, $\langle A(^{95,97}Mo)\rangle$ = 38 G, and $E^1/_2$ = –0.23 and –1.44 V *vs* Fc/Fc⁺ in CH_2Cl_2/0.5 M $Bu_4{}^nNPF_6$; for **2**, $\langle g\rangle = 1.982$, $\langle A\rangle$ = 39 G, and $E^1/_2$ = –0.04 and –1.62 V. All the aforementioned electrochemical processes are quasi-reversible at 25 °C, bulk controlled potential electrolyses affording mixtures of products in all cases. Ferrocenium oxidation of **1** in the presence or absence of H_2O affords salts containing the known ions $[MoO(S_2CNEt_2)_3]^+$ and $[Mo(S_2CNEt_2)_4]^+$, respectively. Extended Hückel MO calculations show that S_2O is both a weaker π-acid and π-base than S_2 in this system and that the electronic structures of **1** and **2** are similar, in agreement with experimental observation, leading to the conclusion that **2** is best considered as a Mo^V complex bearing an $(S_2O)^{2-}$ ligand.

Introduction

The coordination chemistry of the unstable sulfur oxides S_2O and S_2O_2 is still poorly developed.[3,4] Several routes to complexes of these ligands have been devised, such as peracid oxidation of a disulfide complex,[10] nucleophilic attack of H_2S at a coordinated iminooxo-γ^4-sulfane,[13] or *via* the S_2O source 4,5-diphenyl-3,6-dihydro-1,2-dithiin-1-oxide.[14,16] However, only a small number of S_2O or S_2O_2 complexes are known,[3–17] and only six have been structurally characterized, with the S_2O_x (x = 1, 2) ligands binding exclusively in η^2-S,S′ fashion: $[Ir(dppe)_2(S_2O_2)]^+$, $[Mo(S_2CNEt_2)_2(\mu\text{-}S_2O)]_2$,[8] $[Ir(dppe)_2(S_2OMe)]^{2+}$,[9] $[Cp^*Mn(CO)_2(S_2O)]$,[11] $[Cp^*MoO(Me)(S_2O)]$,[15] and $[MoO(S_2CNEt_2)_2(S_2O)]$[16] ($Cp^{*-} = C_5Me_5^-$, dppe = 1,2-bis(diphenylphosphino)ethane). In addition, while an IR study has concluded that S_2O is a better π-acid than S_2,[12] there is uncertainty in the literature as to the electronic character of coordinated S_2O, which has been described by different authors as formally a neutral,[16] uninegative,[8] or dinegative[15] ligand when bound to molybdenum. In this paper, we describe the synthesis of a new S_2O complex $[Mo(S_2O)(S_2CNEt_2)_3]$ (**2**) by oxygen atom transfer to the corresponding S_2 complex $[Mo(S_2)(S_2CNEt_2)_3]$ (**1**). An X-ray crystallographic characterization of **2** has established the structure of this compound, which is the first EPR-active S_2O complex. Also described are EHT MO calculations on **1**, **2**, and the corresponding SO_2 complex that are designed to identify the electronic character of bound S_2O.

Experimental Section

Syntheses. All manipulations were performed using standard inert-atmosphere equipment and Schlenk techniques. Tetraethylthiuram disulfide ($\{Et_2NCS_2\}_2$, Aldrich), $[(C_5H_5)_2Fe]PF_6$ (Aldrich), and 3-chloroperbenzoic acid (mCPBA, Eastman fine chemicals) were used as supplied, while $(^nBu_4N)_2MoS_4$ was prepared by the literature procedure.[18] All solvents were predried and distilled. Elemental microanalyses were performed by Atlantic Microlabs or the Microanalytical Laboratory of the University of Manchester, Manchester, England.

$[Mo(S_2)(S_2CNEt_2)_3]$ (1). This complex was prepared essentially according to the method briefly communicated by Stiefel *et al.*[19] A solution of $(^nBu_4N)_2MoS_4$ (6.00 g, 8.46 mmol) and $\{Et_2NCS_2\}_2$ (6.27 g, 21.0 mmol) in acetonitrile (150 cm³) was stirred at 20 °C for 4 h. The resultant brown precipitate was collected and washed with MeCN (50 cm³) and Et_2O (50 cm³). Recrystallization from CH_2Cl_2/Et_2O afforded large brown crystals of the CH_2Cl_2 solvate of **1**; yield 76%. Anal. Calcd (found) for $C_{15}H_{30}N_3S_8Mo\cdot CH_2Cl_2$: C, 27.9 (28.1); H, 4.68 (4.75); N, 6.1 (6.2); S, 37.2 (37.5). FAB mass spectrum [m/e (%)]: 605 (M⁺ + H, 58), 573 (23), 541 (100), 457 (60), 425 (95). Electronic spectrum in CH_3CN [λ_{max}/nm (ϵ_M/dm³ mol⁻¹ cm⁻¹)]: 434 (sh), 403 (5610), 306 (sh), 263 (46 900), 264 (sh), 218 (35 520). Selected IR data (Nujol mull, cm⁻¹): 1506 (s), 1437 (m), 1356 (m), 1300 (w), 1277 (s), 1209 (m), 1147 (m), 1093 (w), 1076 (m), 1006 (w), 918 (w), 851 (m), 779 (w), 760 (m), 663 (w), 609 (w), 578 (w), 551 (m).

$[Mo(S_2O)(S_2CNEt_2)_3]$ (2). To a solution of **1** (1.65 g, 2.73 mmol) in CH_2Cl_2 (50 cm³), maintained at 0 °C in an ice bath, was added a CH_2Cl_2

® Abstract published in *Advance ACS Abstracts*, August 1, 1994.

(1) Indiana University Chemistry Department.
(2) Indiana University Molecular Structure Center.

(3) Schenk, W. A. *Angew. Chem., Int. Ed. Engl.* **1987**, *26*, 98.
(4) Pandey, K. K. *Prog. Inorg. Chem.* **1992**, *40*, 445.
(5) Schmid, G.; Ritter, G. *Chem. Ber.* **1975**, *108*, 3008.
(6) Lorenz, I.-P.; Kull, J. *Angew. Chem., Int. Ed. Engl.* **1986**, *25*, 261.
(7) Schmid, G.; Ritter, G. *Angew. Chem., Int. Ed. Engl.* **1975**, *14*, 645.
(8) Dirand-Colin, J.; Schappacher, M.; Ricard, L.; Weiss, R. *J. Less-Common Met.* **1977**, *54*, 91.
(9) Hoots, J. E.; Rauchfuss, T. B.; Wilson, S. R. *J. Chem. Soc., Chem. Commun.* **1983**, 1226.
(10) Hoots, J. E.; Lesch, D. A.; Rauchfuss, T. B. *Inorg. Chem.* **1984**, *23*, 3130.
(11) Herberhold, M.; Schmidkonz, B.; Ziegler, M. L.; Zahn, T. *Angew. Chem., Int. Ed. Engl.* **1985**, *24*, 515.
(12) Herberhold, M.; Schmidkonz, B. *J. Organomet. Chem.* **1986**, *308*, 35.
(13) Herberhold, M.; Hill, A. F. *J. Chem. Soc., Dalton Trans.* **1988**, 2027.
(14) (a) Urove, G. A.; Welker, M. E. *Organometallics* **1988**, *7*, 1013. (b) Urove, G. A.; Welker, M. E.; Eaton, B. E. *J. Organomet. Chem.* **1990**, *384*, 105. (c) Powell, K. R.; Elias, W. J.; Welker, M. E. *Ibid.* **1991**, *407*, 81.
(15) Faller, J. W.; Ma, Y. *Organometallics* **1989**, *8*, 609.
(16) Brown, D. S.; Owens, C. F.; Wilson, B. G.; Welker, M. E.; Rheingold, A. L. *Organometallics* **1991**, *10*, 871.
(17) Pandey, K. K. Unpublished results cited in ref 4.
(18) Hadjikyriacou, A. I.; Coucouvanis, D. *Inorg. Synth.* **1990**, *27*, 41.
(19) (a) Pan, W.-H.; Halbert, T. R.; Hutchings, L. L.; Stiefel, E. I. *J. Chem. Soc., Chem. Commun.* **1985**, 927. (b) Harmer, M. A.; Halbert, T. R.; Pan, W.-H.; Coyle, C. L.; Cohen, S. A.; Stiefel, E. I. *Polyhedron* **1986**, *5*, 341.

0020-1669/94/1333-3639$04.50/0

solution of mCPBA (0.47 g, 2.73 mmol). The mixture was stirred for 30 min and then allowed to warm to ambient temperature and filtered. The resultant green solution was concentrated *in vacuo* to 20% of its original volume, and the crude solid product was precipitated with Et_2O. The green-brown solid was collected by filtration, washed with a little DMF, and then recrystallized from CH_2Cl_2/Et_2O to give green microcrystals of the DMF solvate, **2**·DMF; yield 71%. Anal. Calcd (found) for $C_{15}H_{30}N_3S_8OMo·C_3H_7NO$: C, 31.2 (31.3); H, 5.37 (5.36); N, 8.1 (8.1). FAB mass spectrum [*m/e* (%)]: 662 (M^+ + H, 12), 605 (10), 573 (15), 557 (15), 541 (100), 457 (7), 425 (88), 409 (42), 392 (19). Electronic spectrum in CH_3CN [λ_{max}/nm (ϵ_M/dm^3 mol^{-1} cm^{-1})]: 472 (sh), 434 (sh), 405 (5 420), 362 (sh), 308 (sh), 267 (43 760), 242 (sh), 214 (31 470). Selected IR data (Nujol mull, cm^{-1}): 1507 (s), 1434 (m), 1402 (w), 1354 (w), 1300 (w), 1275 (m), 1147 (m), 1089 (m), 1067 (w), 1045 (s), 918 (w), 846 (m), 777 (w), 654 (w), 594 (w), 575 (s), 556 (w), 540 (m), 488 (w).

Conversion of 2 to [Mo(S_2CNEt_2)$_4$](PF_6) (6). Solutions of **2** (0.50 g, 0.83 mmol) and [$(C_5H_5)_2Fe$](PF_6) (0.27 g, 0.83 mmol) in CH_2Cl_2 (50 and 10 cm^3, respectively) were mixed and stirred at ambient temperature for 1 h. The resultant solution was filtered, reduced to 50% of its original volume, and layered with hexanes. This slowly produced a brown material, contaminated with a small number of yellow crystals. Recrystallization of the brown product from CH_2Cl_2/hexanes yielded red-brown needles; yield 50%. Anal. Calcd (found) for $C_{20}H_{40}N_4F_6S_8PMo·{}^1/_2CH_2Cl_2$: C, 28.1 (28.0); H, 4.72 (4.71); N, 6.4 (6.2); S, 29.2 (28.5). FAB mass spectrum [*m/e* (%)]: 689 ($M^+ - PF_6$, 95), 573 (4), 541 (70), 425 (100), 393 (8).

X-ray Crystallography and Structure Solution. Suitable single crystals of **2**·$^1/_2Et_2O$ were grown from $MeNO_2/Et_2O$. Data were collected at −165 °C on a Picker four-circle diffractometer, details of the diffractometry, low-temperature facilities, and computational procedures employed are available elsewhere.[20] The sample was known to lose solvent, so it was kept in contact with its mother liquor until a suitable crystal had been located and transferred to the goniostat for characterization. A small, well-formed crystal was cleaved from a larger sample and affixed to the end of a glass fiber using silicone grease, and the mounted sample was then transferred to the goniostat where it was cooled to −165 °C for characterization and data collection. Standard inert-atmosphere handling techniques were used throughout the investigation. A systematic search of a limited hemisphere of reciprocal space located a set of reflections with monoclinic symmetry and a systematic absences corresponding to a *C*-centered cell with a *c*-glide in the *h*0*l* zone. Subsequent solution and refinement of the structure confirmed the space group to be *C*2/*c*. Data were collected using a standard moving crystal/moving detector technique with fixed background counts at each extreme of the scan. Data were corrected for Lorentz and polarization terms and equivalent data averaged. The structure was solved by direct methods (MULTAN78) and Fourier techniques. All non-hydrogen atoms were readily located, including those of the Et_2O molecule whose oxygen atom lies on a 2-fold rotation axis, and these were refined with anisotropic thermal parameters. A difference Fourier map phased on the non-hydrogen atoms clearly located all hydrogen atoms, and their positional and isotropic thermal parameters were included in the final least-squares refinement cycles. A final difference Fourier map was essentially featureless. Final values of discrepancy indices R and R_w are listed in Table 1.

Physical Measurements. Infrared (Nujol mull) and electronic spectra were recorded on Nicolet 510P and Hewlett-Packard 8452A spectrophotometers, respectively. Positive ion fast atom bombardment (FAB) mass spectra (3-nitrobenzyl alcohol matrix) were obtained using locally constructed instruments which have been described previously.[21] EPR measurements were performed at X-band frequencies (9.4 GHz) on a Bruker ESP300 spectrometer with a Hewlett-Packard 5350B microwave frequency counter. Cyclic voltammograms were recorded with a BAS CV-27 voltammetric analyzer using a standard three-electrode assembly (glassy carbon working, Pt wire auxiliary, SCE reference) with 0.5 M $^nBu_4NPF_6$ as supporting electrolyte. All potentials are quoted versus the ferrocene/ferrocenium couple, at ~20 °C and a scan rate of 100 mV/s. Coulometric determinations were performed with a PAR Model 173 potentiostat, in combination with a Model 179 digital coulometer, using a Pt basket working electrode.

Molecular Orbital Calculations. Calculations were performed using the EHMO method with weighted H_{ij}'s.[22] The parameters for Mo,[23a] S,[23b] C, N, O, and H[23c] were taken from the literature. Atomic coordinates were taken from crystallographic data or generated using CHEM3D[24] from structural parameters given in the literature.[19,30]

Table 1. Crystallographic Data for $Mo(S_2O)(S_2CNEt_2)_3·{}^1/_2Et_2O$ (**2**·$^1/_2Et_2O$)

formula[a]	$C_{17}H_{35}N_3O_{1.5}S_8Mo$
fw	657.95
space group	*C*2/*c*
a, Å	18.294(4)
b, Å	9.468(2)
c, Å	32.101(7)
α, deg	90
β, deg	92.75(1)
γ, deg	90
V, Å^3	5553.94
Z	8
T, °C	−165
radiation[b] (λ, Å)	Mo Kα (0.710 69)
ρ_{calc}, g/cm^3	1.593
μ, cm^{-1}	10.596
octants	+*h*,+*k*,±*l*
total data	4949
unique data	3615
R_{merge}	0.073
obsd data ($F > 2.33\sigma(F)$)	2641
R (R_w)[c]	0.0399 (0.0389)

[a] Including solvate molecule. [b] Graphite monochromator. [c] $R = \sum||F_o| - |F_c||/\sum|F_o|$. [d] $R_w = [\sum w(|F_o| - |F_c|)^2/\sum w/F_o|^2]^{1/2}$, where $w = 1/\sigma^2(|F_o|)$.

Results

Synthesis. We initially came across the new compound [Mo(S_2O)(S_2CNEt_2)$_3$] (**2**) in extremely low yield from the reaction of [MoS_4]$^{2-}$ with [$VCl_2(S_2CNEt_2)_2$], although refinement of the oxygen atom occupancy during crystallographic structure solution gave a value of ~0.60 indicating that **2** and the known[19] [Mo(S_2)(S_2CNEt_2)$_3$] (**1**) had cocrystallized in an approximately

(20) Chisholm, M. H.; Folting, K.; Huffman, J. C.; Kirkpatrick, C. C. *Inorg. Chem.* **1984**, *23*, 1021.
(21) Wong, C. M.; Crawford, R. W.; Barton, V. C.; Brand, H. R.; Neufeld, K. W.; Bowman, J. E. *Rev. Sci. Instrum.* **1983**, *54*, 996.
(22) Ammeter, J. H., Bürgi, H.-B.; Thibeault, J. C.; Hoffmann, R. *J. Am. Chem. Soc.* **1978**, *100*, 3686.
(23) (a) Summerville, R. H.; Hoffmann, R. *J. Am. Chem. Soc.* **1976**, *98*, 7240. (b) Chen, M. M. L.; Hoffmann, R. *Ibid.* **1976**, *98*, 1647. (c) Hoffmann, R. *J. Chem. Phys.* **1963**, *39*, 1397.
(24) CHEM3D Plus version 3.1: Cambridge Scientific Computing, Cambridge, MA, 1992.
(25) (a) Schultz, F. A.; Ott, V. R.; Rolinson, D. S.; Bravard, D. C.; McDonald, J. W.; Newton, W. E. *Inorg. Chem.* **1978**, *17*, 1758. (b) Newton, W. E.; McDonald, J. W.; Yamanouchi, K.; Enemark, J. H. *Ibid.* **1979**, *18*, 1621.
(26) See e.g.: (a) Nieuwpoort, A. *J. Less-Common Met.* **1974**, *36*, 271. (b) McAuliffe, C. A.; Sayle, B. J. *Inorg. Chim. Acta* **1975**, *12*, L7. (c) Kalbacher, B. J.; Bereman, R. D. *Inorg. Chem.* **1975**, *14*, 1417. (d) Pariyadath, N.; Newton, W. E.; Stiefel, E. I. *J. Am. Chem. Soc.* **1976**, *98*, 5388. (e) Hanson, G. R.; Brunette, A. A.; McDonell, A. C.; Murray, K. S.; Wedd, A. G. *Ibid.* **1981**, *103*, 1953. (f) Rajan, O. A.; Spence, J. T.; Leman, C.; Minelli, M.; Sato, M.; Enemark, J. H.; Kroneck, P. M. H.; Sulger, K. *Inorg. Chem.* **1983**, *22*, 3065. (g) Chaudhury, M. *Polyhedron* **1986**, *5*, 387. (h) Chang, C.-S. J.; Enemark, J. H. *Inorg. Chem.* **1991**, *30*, 683.
(27) Müller, A.; Jaegermann, W.; Enemark, J. H. *Coord. Chem. Rev.* **1982**, *46*, 245.
(28) (a) Leonard, K.; Plute, K.; Haltiwanger, R. C.; Rakowski-Dubois, M. *Inorg. Chem.* **1979**, *18*, 3246. (b) McDonald, J. W.; Newton, W. E. *Inorg. Chim. Acta* **1980**, *44*, L81. (c) Young, C. G.; Boreham, C. J.; Broomhead, J. A. *J. Chem. Soc., Dalton Trans.* **1983**, 2135.
(29) (a) Brennan, T. F.; Bernal, I. *Inorg. Chim. Acta* **1973**, *7*, 283. (b) March, F. C.; Mason, R.; Thomas, K. M. *J. Organomet. Chem.* **1975**, *96*, C43. (c) Dirand, J.; Ricard, L.; Weiss, R. *Transition Met. Chem.* **1975/76**, *1*, 2. (d) Bishop, M. W.; Chatt, J.; Dilworth, J. R.; Hursthouse, M. R.; Motevalle, M. *J. Less-Common Met.* **1977**, *54*, 487. (e) Butler, G.; Chatt, J.; Leigh, G. J.; Smith, A. R. P.; Williams, G. A. *Inorg. Chim. Acta* **1978**, *28*, L165. (f) Butler, G.; Chatt, J.; Hussain, W.; Leigh, G. J.; Hughes, D. L. *Ibid.* **1978**, *30*, L287. (g) Bishop, M. W.; Chatt, J.; Dilworth, J. R.; Neaves, B. D.; Dahlstrom, P.; Hyde, J.; Zubieta, J. *J. Organomet. Chem.* **1981**, *213*, 109. (h) Broomhead, J. A.; Sterns, M.; Young, C. G. *J. Chem. Soc., Chem. Commun.* **1981**, 1262. (i) Dupré, N.; Hendriks, H. M. J.; Jordanov, J. *J. Chem. Soc., Dalton Trans.* **1984**, 1463.
(30) Broomhead, J. A.; Gill, N. S.; Hammer, B. C.; Sterns, M. *J. Chem. Soc., Chem. Commun.* **1982**, 1234.

3:2 ratio. As **1** is a known compound and since we had decided to pursue development of a rational and high-yield route to pure **2** to allow detailed characterization of this novel compound, potential means of converting **1** to **2** were considered. The first attempted was oxygen atom transfer from 3-Cl-$C_6H_4CO_3H$ (mCPBA), and this proved successful. Thus, treatment of **1** with 1 equiv of mCPBA in CH_2Cl_2 at 0 °C, followed by solvent removal *in vacuo*, washing of the solid with DMF to remove excess reagents and some side products, and recrystallization from CH_2Cl_2/Et_2O, gave high yields (typically ~70%) of green-brown crystals. The IR spectrum of the crystals showed bands at 1507, 1045, and 540 cm^{-1}, assignable to C–N, S–O, and S–S stretching vibrations, respectively, supporting attainment of the desired S_2O complex. Elemental analysis and FAB mass spectral data were consistent with the formulation **2**·DMF. An analogous reaction at 20 °C gave greatly reduced yields of **2** (~20%) and much more intensely colored DMF washings; layering of the latter with Et_2O gave yellow crystals identified as the known dinuclear complex $[Mo_2(O)(S)(\mu\text{-}S)_2(S_2CNEt_2)_2]$.[25] The conversion of **1** to **2** is summarized in eq 1. As described above, available data supported

$$\underset{\mathbf{1}}{[Mo(S_2)(S_2CNEt_2)_3]} \xrightarrow{[O]} \underset{\mathbf{2}}{[Mo(S_2O)(S_2CNEt_2)_3]} \quad (1)$$

the indicated formulation of **2**, but a definitive structural characterization proved elusive owing to the poor diffraction qualities of crystals from CH_2Cl_2/Et_2O; however, crystals grown from a $MeNO_2/Et_2O$ layering of formulation $\mathbf{2}\cdot{}^1/_2Et_2O$ were found to be good diffractors, allowing structural characterization (*vide infra*). Complex **2** is air stable in the solid state and can be recovered from organic solvents after several days at ambient temperature. However, it does appear to slowly revert to **1** in MeCN and CH_2Cl_2 solution, as evidenced by the ingrowth of weak signals attributable to **1** in the EPR spectrum and cyclic voltammogram of **2** within minutes of dissolution of pure crystalline samples of **2** in these solvents. Attempts to prepare $[Mo(S_2O_2)(S_2CNEt_2)_3]$ by reaction of 2 equiv of mCPBA with **1** were unsuccessful, again affording only reduced yields of **2**.

Description of Structure. An ORTEP representation of complex **2** is shown in Figure 1. Selected atomic coordinates and interatomic distances and angles are listed in Tables 2 and 3, respectively. Complex $\mathbf{2}\cdot{}^1/_2Et_2O$ crystallizes in monoclinic space group *C*2/*c* with the $[Mo(S_2O)(S_2CNEt_2)_3]$ molecule having no crystallographically-imposed symmetry. The Mo atom is ligated by three chelating $Et_2NCS_2^-$ groups and a η^2-S_2O group bound through its S atoms. The Mo is thus seven-coordinate (assuming S_2O occupies a single site) and possesses distorted pentagonal bipyramidal geometry with S(21) and S(2)/S(3) in the axial sites. The latter geometry is common to all structurally-characterized $[MoX(S_2CNR_2)_3]^{n+}$ complexes (X = NO, NS, HS^-, N^{3-}, $R'NN^-$, η^2-S_2^{2-} (**1**), η^2-SO_2 (**3**) (n = 0); X = O^{2-}, $R'N^{2-}$, R'_2NN^{2-} (n = 1)).[19,29,30] The S_2O group in **2** is ligated in the asymmetric, side-on η^2-fashion observed for other S_2O complexes. Compared to free S_2O, the S–S and S–O bonds are slightly lengthened and the S–S–O angle slightly contracted. The structural parameters for free S_2O and the bound S_2O group in a number of complexes are listed for comparison in Table 4. The M–S distances are all within the range 2.3–2.5 Å, and in every case the S–S bonds (2.011(3)–2.100(5) Å) are longer than in free S_2O (1.884 Å) and the O–S–S angles are *very* slightly smaller (113.3(3)–117.4(6)°) than in free S_2O (118°) except for $[Ir(S_2OMe)(dppe)_2]^{2+}$, where the more pronounced decrease in O–S–S angle is caused by methylation of the S_2O oxygen atom. The S–O bond in **2** points slightly away from the equatorial plane of

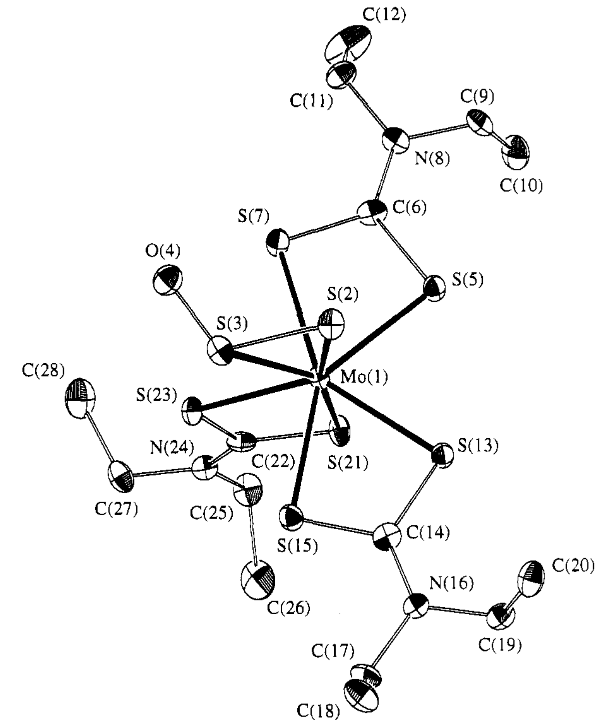

Figure 1. ORTEP representation of complex **1** at the 50% probability level.

Table 2. Fractional Coordinates (×10⁴)[a] and Equivalent Isotropic Thermal Parameters (Å² × 10)[b] for $Mo(S_2O)(S_2CNEt_2)_3\cdot{}^1/_2Et_2O$ ($\mathbf{2}\cdot{}^1/_2Et_2O$)

atom	*x*	*y*	*z*	B_{eq}
Mo(1)	7964.3(3)	367(1)	1171.8(2)	11
S(2)	9001(1)	1339(2)	821(1)	17
S(3)	9187(1)	1280(2)	1445(1)	16
O(4)	9183(2)	2678(5)	1665(2)	20
S(5)	7197(1)	1441(2)	578(1)	14
C(6)	7097(3)	2951(7)	864(2)	15
S(7)	7521(1)	2794(2)	1347(1)	15
N(8)	6747(3)	4087(6)	718(2)	14
C(9)	6373(4)	4071(8)	300(2)	17
C(10)	5634(4)	3373(9)	288(2)	23
C(11)	6710(4)	5395(8)	962(2)	19
C(12)	5937(4)	5806(9)	1052(3)	33
S(13)	7928(1)	−1380(2)	571(1)	14
C(14)	8448(3)	−2539(7)	867(2)	14
S(15)	8633(1)	−1869(2)	1356(1)	16
N(16)	8646(3)	−3807(6)	742(2)	13
C(17)	9040(4)	−4794(8)	1025(2)	17
C(18)	9827(4)	−5051(8)	909(2)	24
C(19)	8454(4)	−4925(7)	315(2)	17
C(20)	8958(4)	−3715(9)	−8(2)	22
S(21)	6782(1)	−700(2)	1369(1)	15
C(22)	7055(3)	−533(7)	1884(2)	14
S(23)	7912(1)	233(2)	1945(1)	14
N(24)	6668(3)	−880(6)	2205(2)	13
C(25)	5922(4)	−1471(8)	2144(2)	19
C(26)	5914(4)	−3055(10)	2191(3)	32
C(27)	6946(4)	−711(8)	2634(2)	18
C(28)	6806(4)	743(9)	2803(2)	26
O(29)	5000*	2314(8)	2500*	26
C(30)	5275(5)	3149(10)	2178(3)	36
C(31)	5542(5)	2212(11)	1847(3)	40

[a] Parameters marked with an asterisk were not varied. [b] Calculated using the formula given by: Hamilton, W. C. *Acta Crystallogr.* **1959**, *12*, 609.

(31) Meschi, D. J.; Myers, R. J. *J. Mol. Spectrosc.* **1959**, *3*, 405.
(32) (a) Nieuwpoort, A.; Moonen, J. H. E.; Cras, J. A. *Recl. Trav. Chim. Pays-Bas* **1973**, *92*, 1086. (b) Nieuwpoort, A. *J. Less-Common Met.* **1974**, *36*, 271. (c) McAuliffe, C. A.; Sayle, B. J. *Inorg. Chim. Acta* **1975**, *12*, L7. (d) Nieuwpoort, A.; Steggerda, J. J. *Recl. Trav. Chim. Pays-Bas* **1976**, *95*, 250. (e) Garner, C. D.; Howlader, N. C.; Mabbs, F. E.; McPhail, A. T.; Miller, R. W.; Onan, K. D. *J. Chem. Soc., Dalton Trans.* **1978**, 1582. (f) Jasim, K. S.; Umbach, G. M.; Chieh, C.; Mak, T. C. W. *J. Crystallogr. Spectrosc. Res.* **1985**, *15*, 271.
(33) Bond, A. M.; Martin, R. L. *Coord. Chem. Rev.* **1984**, *54*, 23.

Table 3. Selected Bond Distances (Å) and Angles (deg) for $Mo(S_2O)(S_2CNEt_2)_3 \cdot {}^1/_2Et_2O$ ($2 \cdot {}^1/_2Et_2O$)

(a) Bonds

Mo(1)–S(2)	2.4320(18)	Mo(1)–S(15)	2.5018(9)
Mo(1)–S(3)	2.5172(18)	Mo(1)–S(21)	2.4959(18)
Mo(1)–S(5)	2.5259(18)	Mo(1)–S(23)	2.4933(18)
Mo(1)–S(7)	2.5102(19)	S(2)–S(3)	2.0169(25)
Mo(1)–S(13)	2.5398(19)	S(3)–O(4)	1.500(5)

(b) Angles

S(2)–Mo(1)–S(3)	48.06(6)	S(5)–Mo(1)–S(21)	84.09(6)
S(2)–Mo(1)–S(5)	85.18(6)	S(5)–Mo(1)–S(23)	136.48(6)
S(2)–Mo(1)–S(7)	91.43(6)	S(7)–Mo(1)–S(13)	140.34(6)
S(2)–Mo(1)–S(13)	83.53(6)	S(7)–Mo(1)–S(15)	151.80(6)
S(2)–Mo(1)–S(15)	92.68(6)	S(7)–Mo(1)–S(21)	91.15(6)
S(2)–Mo(1)–S(21)	167.12(6)	S(7)–Mo(1)–S(23)	78.13(6)
S(2)–Mo(1)–S(23)	123.26(6)	S(13)–Mo(1)–S(15)	67.86(6)
S(3)–Mo(1)–S(5)	125.26(6)	S(13)–Mo(1)–S(21)	86.43(6)
S(3)–Mo(1)–S(7)	84.18(6)	S(13)–Mo(1)–S(23)	136.30(6)
S(3)–Mo(1)–S(13)	118.63(6)	S(15)–Mo(1)–S(21)	90.99(6)
S(3)–Mo(1)–S(15)	78.01(6)	S(15)–Mo(1)–S(23)	76.31(6)
S(3)–Mo(1)–S(21)	144.80(6)	S(21)–Mo(1)–S(23)	69.62(5)
S(3)–Mo(1)–S(23)	75.29(6)	Mo(1)–S(2)–S(3)	68.18(7)
S(5)–Mo(1)–S(7)	68.08(6)	Mo(1)–S(3)–S(2)	63.76(7)
S(5)–Mo(1)–S(13)	72.29(6)	Mo(1)–S(3)–O(4)	116.23(19)
S(5)–Mo(1)–S(15)	140.08(6)	S(2)–S(3)–O(4)	116.00(22)

the complex, the Mo–S(2)–S(3)–O(4) torsion angle being 108°. The bond angles and distances within the $[Mo(S_2CNEt_2)_3]$ fragment are unexceptional. Overall, the molecular geometry of **2** is almost identical to that of $[Mo(SO_2)(S_2CNEt_2)_3]$ (**3**), which differs only in the identity of one atom.[30]

Two further comparisons in Table 4 deserve comment. First, the Mo–S and S–S bonds in **2** are longer and shorter, respectively, than for the other Mo–S_2O complexes. However, given the (relatively) short S–S bond, the S–O distance in **2** seems unusually long; it has been suggested that S–S and S–O should both increase on coordination to a metal, owing to M→S_2O π-back-donation.[16] Second, the Mo–S distances in **2** are noticeably longer than in **1**, while the S–S distance in **2** is slightly shorter than in **1** (but approximately equal by the 3σ criterion). This again is slightly surprising since S_2O is generally considered a better π-acid than S_2,[12] and it might have been expected to give the shorter Mo–S and noticeably longer S–S bonds. Further consideration of these points will be provided below.

EPR Spectroscopy. The X-band EPR spectra of **1** and **2** in fluid CH_2Cl_2 solution at 298 K are similar, both showing a $g \approx 2$ signal and a six-line satellite signal from hyperfine interactions with $^{95,97}Mo$ nuclei ($I = {}^5/_2$, 25% abundance) (Figure 2). These spectra are as expected for $S = {}^1/_2$ systems. The observed g_{iso} and A_{iso} values (**1**, $g_{iso} = 1.977$, $A_{iso} = 38$ G; **2**, $g_{iso} = 1.982$, $A_{iso} = 39$ G) are typical for Mo^V centers in a sulfur-rich ligand environment.[26] In a frozen CH_2Cl_2 glass at 77 K, broad resonances are seen at g values identical to those in fluid solution. In a CH_2Cl_2:toluene (1:1) glass at 10 K, the spectra, while still relatively broad, display effective axial symmetry but no resolvable $^{95,97}Mo$ hyperfine splitting (**1**, $g_\parallel = 1.993$, $g_\perp = 1.974$; **2**, $g_\parallel = 2.003$, $g_\perp = 1.976$).

Complex **1** is generally regarded as a Mo^V complex containing a dianionic S_2^{2-} ligand; the near congruence of the two EPR

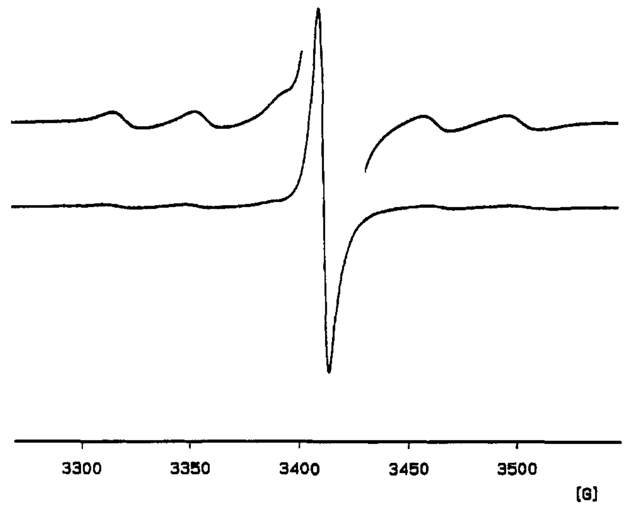

Figure 2. X-band EPR spectrum of $[Mo(S_2CNEt_2)_3(S_2O)]$ (**2**) in CH_2Cl_2 at 298 K.

spectra suggest that **2** is thus best described as a Mo^V complex with a S_2O^{2-} ligand. Although the disulfur group bound to a metal is generally considered as a persulfido (S_2^{2-}) moiety,[27] and ionic S_2^{2-} salts are readily isolable, uncomplexed S_2O exists only as an (unstable) neutral molecule in the gas phase. In light of the conclusion that **2** contains a bound S_2O^{2-} group, it is interesting to note that the S–S distance in **2** is essentially identical to that in $[Ir(S_2OMe)(dppe)_2]^{2+}$, which is clearly best described as an Ir^{III} complex bearing an S_2OMe^- ligand, formed by attack of Me^+ on an S_2O^{2-} group, rather than an Ir^I complex with a S_2OMe^+ group;[9] the S–O distance in this species is longer, however, than in **2**, as expected from the methylation of the S_2O^{2-} oxygen atom.

Electrochemical Studies. Both **1** and **2** display one quasi-reversible oxidation and one quasi-reversible reduction when investigated by cyclic voltammetry (CV) at 20 °C at 100 mV/s in CH_2Cl_2 solution under Ar containing 0.5 M $NBu_4{}^nPF_6$. The potentials, *vs* Cp_2Fe/Cp_2Fe^+, for **1** were −0.23 V ($\Delta E_p = 255$ mV, $E_p^f/E_p^r = 0.62$) and −1.44 V ($\Delta E_p = 190$ mV, $E_p^f/E_p^r = 0.95$), and for **2** they were −0.04 V ($\Delta E_p = 240$ mV, $E_p^f/E_p^r = 0.90$) and −1.62 V ($\Delta E_p = 300$ mV, $E_p^f/E_p^r = 0.96$). The data were suggestive of unstable oxidation and reduction products; coulometry experiments gave a value of $n \approx 1$ for the oxidation of **1** but $n > 1$ for the other three processes. Controlled potential electrolyses were performed in both the oxidizing and reducing directions for **1** and **2**, and the four experiments all gave brown solutions that displayed complex CV traces suggesting the presence of mixtures of products; in no case was regeneration of starting material observed on switching the potential to the appropriate value, confirming that oxidized and reduced **1** and **2** have irreversibly converted to other chemical species. Significantly, the CV's of oxidized and reduced solutions of **1** were identical to those of **2**. Although it is difficult to safely identify from the CV traces of electrolyzed solutions the identity of the mixtures of products present, nevertheless we note that they are similar to

Table 4. Comparative Structural Data for Free S_2O and Metal–S_2O Complexes

	M–S (M–O) (Å)	S–S (Å)	S–O (Å)	O–S–S (deg)	ref
Free S_2O		1.884	1.465	118	31
$[Mo(S_2)(S_2CNEt_2)_3]$ (**1**)	2.418(2), 2.445(2)	2.022(3)			19
$[Mo(S_2O)(S_2CNEt_2)_3)]$ (**2**)	2.432(2), 2.517(2)	2.017(3)	1.500(5)	116.0(2)	this work
$[Mo(SO_2)(S_2CNEt_2)_3]$ (**3**)	2.149(8),[a] 2.463(4)		1.440(11), 1.506(9)[b]	114.5(6)[c]	30
$[MoO(S_2O)(S_2CNEt_2)_2]$	2.401(1), 2.500(1)	2.029(1)	1.454(4)	114.3(1)	16
$[Cp^*MoO(S_2O)(Me)]$	2.307(2), 2.500(2)	2.050(3)	1.482(6)	113.3(3)	15
$[Cp^*Mn(S_2O)(CO)_2]$	2.328(5), 2.400(5)	2.013(8)	1.521(13)	117.4(6)	11
$[Mo(\mu\text{-}S_2O)(S_2CNEt_2)_2]_2$[d]	2.365(3), 2.397(3), 2.472(3)	2.100(5)	1.482(9)	115.7(4)	8
$[Ir(S_2OMe)(dppe)_2]^{2+}$	2.368(2), 2.431(2)	2.011(3)	1.619(8)	109.6(3)	9

[a] M–O bond distance. [b] S–O bond distance for bound S and O atoms. [c] O–S–O angle. [d] Average values for two S_2O ligands.

those reported for $[Mo(S)_2(S_2CNEt_2)_2]$, $[Mo_2(S)_2(\mu\text{-}S)_2(S_2CNEt_2)_2]$, and related Mo oxo– and Mo sulfide–dithiocarbamate species.[25a,34]

In an attempt to more securely identify a redox product of these complexes, chemical oxidation of complex **1** was carried out on a preparative scale. Treatment of **1** with 1 equiv of $[Cp_2Fe](PF_6)$ in CH_2Cl_2 under N_2 at 20 °C afforded a green solution from which the known yellow compound $[MoO(S_2CNEt_2)_3](PF_6)$ (**4**)[28,29c,d] was isolated in 65% yield by crystallization with Et_2O, together with small amounts of a blue-green complex (**5**, estimated yield ~15%) that we have yet to characterize. Complex **4** was identified by microanalysis and by comparison of its spectroscopic properties (UV/vis, IR) with those previously reported for this complex. The oxygen atom presumably arises from nucleophilic attack by H_2O (undoubtedly originating from the $[Cp_2Fe](PF_6)$, which is hygroscopic) on $\mathbf{1}^+$ with the elimination of S_2^{2-}.

$$\underset{\mathbf{1}^+}{[Mo(S_2)(S_2CNEt_2)_3]^+} + H_2O \rightarrow \underset{\mathbf{4}}{[MoO(S_2CNEt_2)_3]^+} + 2H^+ + S_2^{2-} \quad (2)$$

An identical reaction using freshly-dried $[Cp_2Fe](PF_6)$ produced instead a brown solution from which, in addition to now small amounts (~10%) of yellow and green solids, was isolated red-brown crystals of known $[Mo(S_2CNEt_2)_4](PF_6)$ (**6**)[32] in ~50% yield on addition of hexanes. The formation of **6** is difficult to rationalize in detail, but it is presumably one of several species in an equilibrium mixture of the type known to exist in oxidized Mo–dithiocarbamate solutions.[33,34] Complex **6** was identified by spectroscopic (EPR, UV/vis, IR) comparison with authentic material reported in the literature and by elemental analysis and FAB mass spectrometry. Complex **6** is air- and water-stable and is therefore not an intermediate in the formation of **4**.

Extended Hückel Molecular Orbital Calculations. In order to rationalize the unexpected similarity in spectroscopic and redox properties of **1** and **2**, and to better understand the electronic character of the Mo–S_2O bond, EHT MO calculations were performed on $[Mo(S_2CNH_2)_3X]$ (X = S_2 (**1′**), S_2O (**2′**), SO_2 (**3′**)); for the purposes of this discussion $[Mo(S_2CNH_2)_3]$, S_2, S_2O, and SO_2 are all treated as neutral fragments. While a detailed analysis of the Mo–X bonding in these molecules is complicated by extensive orbital mixing within the $[Mo(S_2CNH_2)_3]$ fragment, it is clear that X→Mo σ- and π-donation and Mo→X back-donation are involved (Figures 3–5). The singly occupied orbitals (SOMO) in **1′** and **2′** are very similar, possessing $Mo(d_{xz})$–$S_2(\psi_3)$ and $Mo(d_{xz})$–$S_2O(\psi_4)$ antibonding character, respectively; this overlap is nonzero owing to the asymmetric η^2-binding of S_2 and S_2O to the Mo center. Each SOMO is well isolated from its corresponding HOMO [ΔE(HOMO–SOMO) = 0.42 eV for **1′** and 0.69 eV for **2′**] and LUMO [ΔE(LUMO–SOMO) = 1.80 eV for **1** and 2.04 for **2′**]. The similar electronic structures and isolated ground states account for the similar room-temperature EPR behaviors of **1** and **2**. Interestingly, comparison of the electron populations of the S_2O and S_2 fragment orbitals in **1′** and **2′** with those in the free ligands shows that, on coordination to the $[Mo(S_2CNH_2)_3]$ unit, the π-donor orbital of S_2 (ψ_3) is depopulated and the acceptor orbital (ψ_2) is populated, to a greater extent than the corresponding orbitals of S_2O (ψ_4 and ψ_3, respectively). This is consistent with the relative energies of these orbitals in free S_2O and S_2 and implies that of the two ligands S_2 is both the better π-acid *and* the better π-base. The difference in acceptor capability between these two ligands as expressed in the fragment orbital electron populations is small, however, and the π-donation effect dominates the difference overall. Hence, these calculations suggest that previous observations interpreted as indicating S_2O to be a better π-acid than S_2 are implying rather that S_2 is a better π-base than S_2O.

A study of the variation of Mo–S_2O overlap and overall

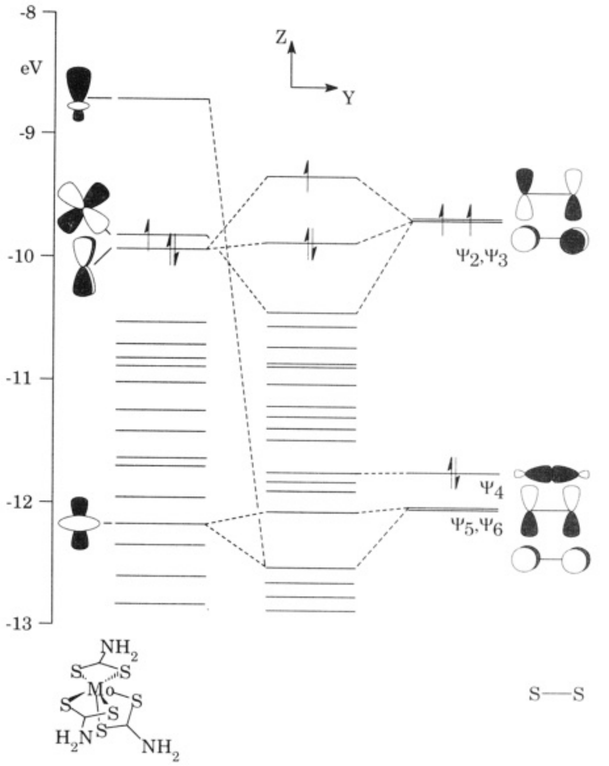

Figure 3. MO diagram for complex **1′** and its constituent fragments. Only those orbitals most important to Mo–S_2 bonding considerations are depicted.

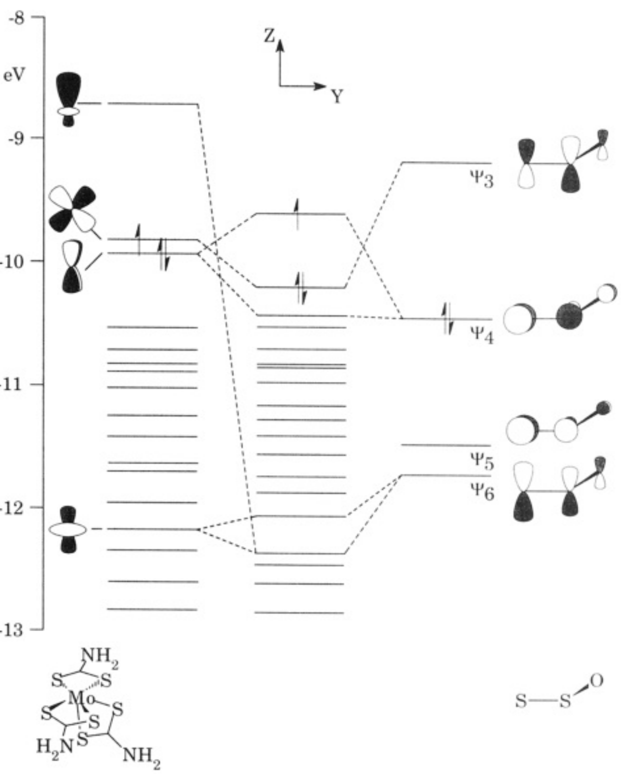

Figure 4. MO diagram for complex **2′** and its constituent fragments. Only those orbitals most important to Mo–S_2O bonding considerations are depicted.

(34) (a) de Hayes, L.; Faulkner, H. C.; Doub, W. H., Jr.; Sawyer, D. T. *Inorg. Chem.* **1975**, *14*, 2410. (b) Faulkner, H. C. *J. Electrochem. Soc.* **1978**, *125*, 287C. (c) Miller, K. F.; Bruce, A. E.; Corbin, J. L.; Wherland, S.; Stiefel, E. I. *J. Am. Chem. Soc.* **1980**, *102*, 5102. (d) Nagaraja, K. S.; Udupa, M. R. *Polyhedron* **1985**, *4*, 649.

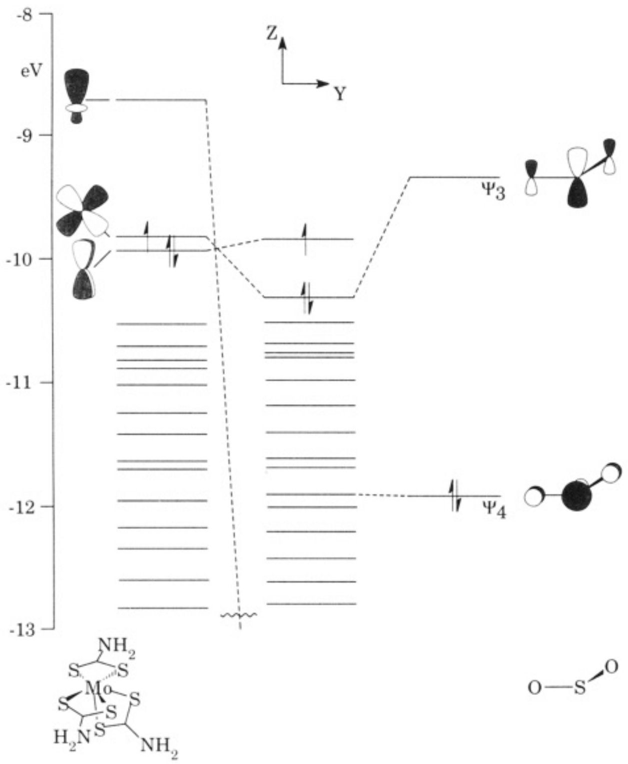

Figure 5. MO diagram for complex **3′** and its constituent fragments. Only those orbitals most important to Mo–SO_2 bonding considerations are shown.

electronic energy with increasing Mo–S–S–O torsion angle (Θ) for **2′** gave a broad energy minimum between Θ = 98 and 110° (*cf.* for **2**, Θ = 108° by X-ray diffraction), with a maximum energy difference of +1.2 eV for Θ = 180°. The "side-on" coordination of the S_2O ligand maximizes σ-overlap of ψ_3 with d_{yz} of the Mo center, thus facilitating Mo→S_2O back-bonding: on rotation of the S_2O ligand about the S–S vector this interaction is replaced by a destabilizing filled–filled Mo(d_{yz})–S_2O(ψ_4) overlap. The asymmetric nature of the Mo–S_2O bond (i.e., Mo–S(3) > Mo–S(2)) is difficult to rationalize in terms of orbital overlap alone, since the largest orbital coefficient for ψ_3 of S_2O lies on central S(3) rather than S(2), and probably occurs for coulombic reasons because of the high positive charge on S(3) (+0.73 in free S_2O by SCF calculation).[35]

In comparison with S_2O, the σ-donor π_z (ψ_6 and ψ_9, not shown) and π-donor π_y^* (ψ_4) orbitals of free SO_2 lie much lower in energy,[35] so that donation from these plays relatively little part in Mo–SO_2 bonding in **3′** (Figure 5). The dominant interaction in this complex is Mo(d_{yz})→SO_2(ψ_3) back-donation, which is similar in magnitude to that observed in **1′** and **2′**: this is consistent with the η^2-SO_2 bonding mode observed for this complex, which only occurs to electron-rich metal centers.[36] The SOMO for **3′** is a nonbonding Mo(d_{xz}) orbital, with a HOMO–SOMO gap of 0.45 eV, implying that **3** should also have an $S = {}^1/_2$ ground state and hence be EPR-active, although this prediction remains to be verified by experiment.

Although calculations of this type cannot unambiguously assign oxidation states to metal and ligand centers, it is clear from the similar populations of the S_2 (ψ_2), S_2O (ψ_3), and SO_2 (ψ_3) π_z^*-LUMOs in **1′**, **2′**, and **3′** that substantial Mo→X charge transfer occurs in these complexes and that the charge distribution in all three compounds is similar. Therefore, while such formalisms are of limited value for a complex high in soft, π-bonding ligands, given the observed EPR and redox properties of **1** and **2**, it is reasonable to class **2** as a Mo^V complex bearing an S_2O^{2-} ligand.

Acknowledgment. This work was supported by the Office of Basic Energy Sciences, Division of Chemical Sciences, U.S. Department of Energy, under Grant DE-FG02-87ER13702. The authors thank Dr. John G. Reynolds (Lawrence Livermore) for contributions to the initial stages of this work, Michael W. Wemple (Indiana University) for the EPR spectra, and Professor Odile Eisenstein (Laboratoire de Chimie Théorique, Centre de Paris-Sud, Orsay, France) for helpful discussions.

Supplementary Material Available: Textual and tabular summaries of the structure determination, tables of atomic coordinates, thermal parameters, and bond distances and angles, and a figure with atom numbering for **2**·${}^1/_2Et_2O$ (13 pages). Ordering information is given on any current masthead page.

(35) Bock, H.; Solouki, B.; Rosmus, P.; Steudel, R. *Angew. Chem., Int. Ed. Engl.* **1973**, *12*, 933.

(36) (a) Mingos, D. M. P. *Transition Met. Chem.* **1978**, *3*, 1. (b) Ryan, R. R.; Kubas, G. J.; Moody, D. C.; Eller, P. G. *Struct. Bonding (Berlin)* **1981**, *46*, 47.